

Engineering Sulfur-Doped Graphene through Chemical Vapor Deposition for Enhanced Electrochemical Sensing of Dopamine and Ascorbic Acid

Dronavalli Bhargavi^{1*}, Ande Rajesh⁴, Vallabhaneni Madhava Rao^{2*}, G.V. Adilakshmi³ and Kolli Deepthi⁴

1. Department of Chemistry, Acharya Nagarjuna University, Guntur, Andhra Pradesh, INDIA

2. Department of Chemistry (recognized as Research Centre by A. N. University), Bapatla Engineering College (Autonomous), Bapatla, Andhra Pradesh, INDIA

3. Department of Chemistry, NRI Institute of Technology, Agiripally, Andhra Pradesh, INDIA

4. Department of Chemistry, Koneru Lakshmaiah Education Foundation, Green fields, Vaddeswaram, Guntur-522502, Andhra Pradesh, INDIA

*bhargavi091985@gmail.com; vmrgpm@gmail.com

Abstract

Here the present work briefly discussed the synthesis of sulfur-doped graphene (SDG) for accurate determination of individual and simultaneous quantification of ascorbic acid (AA) and dopamine (DA). SDG catalyst material was prepared by using a hydrothermal technique using a carbon and sulfur source. The structural properties of SDG and its associated materials are examined using Raman spectroscopy; FT-IR analysis and morphological studies were examined using high-end FE-SEM and HR-TEM, atomic force microscopy and water contact angle dimensions.

Further, SDG material-modified glassy carbon electrode (SDG/GCE) is employed to estimate the accurate quantification of DA and AA experienced through cyclic voltammetry, as well as chronoamperometry to examine the charge transfer properties at SDG. The modified electrode SDG/GCE showed finite selectivity, sensitivity and low limit of detection, with a regression coefficient value of 0.99 for DA and AA correspondingly. On the other hand, the proposed has finite stability with a retention capacity of almost 95 % after 12 days.

Keywords: Amperometry, Ascorbic acid, Cyclic voltammetry, Dopamine, Sulfur-doped graphene, Ascorbic acid.

Introduction

Dopamine (DA) is a neuromodulator molecule that employs an imperative function in cells as well as physiological processes in human metabolism, cardiovascular and central nervous systems^{12,13,33}. Lack or inefficiency of DA in the human body is severely the cause of many diseases and neurological disorders^{25,30,32,34}. Further study of its electrochemical properties and estimations of this molecule in human body fluids is essential. DA is easily oxidized at conventional electrode surfaces and these are used for quantification in *in vivo* and *in vitro* studies. AA is one type of polyhydroxy material and it has having similar structure to glucose⁶. AA is a familiar compound of its antioxidant

properties and generally coexists with the DA metabolism system^{2,35,40}.

AA mainly affects physiological observations and has utility of detoxification, cancer deterrence, along with the minimization of scurvy^{18,20,38}. DA and AA both these compounds are both electroactive and electrochemically oxidized at the electrode surface. The electrochemical quantification of these molecules, individual and simultaneous, is receiving considerable attention. However, the quantification of these molecules at bare electrodes has high over-potential and low current density. Further, during the electro-oxidation of these molecules, the electrode surfaces are easily undergoing electrode fouling^{5,36}.

In addition to this, the main drawback of the electrochemical estimation of DA is the intrusion from AA. It is mainly due to the oxidation potentials of DA along with AA being extremely close to each other at traditional electrodes, for example, Au, Pt and glassy carbon electrodes (GCE)⁷. The product of DA oxidation can also participate in the electrochemical oxidation of AA, this reaction may signify the electrode fouling with minimal selectivity and generability²¹. For that reason, the careful estimation of DA in the occurrence of AA is a foremost challenging issue¹⁵.

To relieve these issues for accurate observation of DA and AA individually and simultaneously, a series of different nanomaterials for instance organic redox mediators, nanomaterials, polymers and self-accumulated monolayers have been used^{4,28,29,41,43}. Carbon-based electrodes have been employed in the instantaneous electrochemical determination of AA and DA over the past two decades^{3,14,16,24,27,39,44}. However, in the present work, we synthesized SDG with a simple and reliable chemical route followed by completely explored microscopic and electrochemical techniques. Later this material-modified GCE is used for quantification of individual and simultaneous AA and DA molecules.

The results showed that the SDG/GCE showed excellent activity with finite selectivity and sensitivity. These are the characteristic properties of biosensors which are powerful tools to detect biomolecules in real time. This capability makes them essential in different fields including food safety, environmental monitoring, medical diagnosis and biotechnology¹¹.

*Author for Correspondence

Material and Methods

Materials: The chemicals are procured with national and international chemical suppliers with AR grade. Dopamine, H_3PO_4 , HNO_3 , H_2SO_4 , NaOH and CH_3COOH were procured from SRL Chemical Company. Graphite material was obtained from Alfa Aesar. DA, AA, DMF and Na_2S were acquired from research laboratories of SISCO, India. The whole required solutions were prepared with $18\ M\Omega\cdot cm$ resistivity containing ultra-pure water.

Electrochemical Measurements: All the electrochemical experiments were carried by AMETEK electrochemical workstation using an electrode system. SDG/GCE worked as a working electrode, platinum mesh and Ag/AgCl electrode served as counter electrodes and standard correspondingly. This electrode system is experienced for whole electrochemical conduct experiments and carried at ambient room temperature in 0.1M PBS (phosphate buffer) with pH 7.0.

Spectroscopic Characterizations: The structural and morphological features of prepared SDG materials are thoroughly examined with FE-SEM using Vega3 Tescan model. HR-TEM studies are carried out at 200kV with a FEI Technai G2 S-Twin. Functional groups were examined using FT-IR spectroscopy with Nexus 670 model FTIR spectrometer. Renishaw Invia Raman Microscope was used to study the Raman analysis using He-Ne Laser 633 nm, 18 mW. The elemental composition of synthesized material was examined with Multilab 2000 thermo scientific XPS spectroscopy. Atomic force microscopy analysis was carried out with Agilent 5500 AFM.

Synthesis of Sulfur Doped Graphene (SDG): The SDG nanomaterial was prepared by using a hydrothermal route using pre-synthesized Graphene oxide (GO)¹⁷ and Na_2S material. These materials served as sources of carbon and sulfur. Initially, 5g of GO and 5g of Pluronic F-127 were added separately in 100 ml deionized water. Stand for 1 hr under ultrasound irradiation. After completion of the reaction, 10mM of sodium sulfide solution was slowly added to the above-mentioned reaction solution and make up to 300 ml. Later for the doping of S, whole reaction mixture was allowed to stand for 2 hr under ultrasound irradiation and subsequently shifted to hydrothermal autoclaves. Keep this vessel in the hydrothermal chamber and operate at 200°C for 12h followed by the SDG. Place in vacuum furnace for 10h at 80°C and the resulted SDG material was used for further physical characterization and electrochemical sensor analysis studies.

Results and Discussion

Morphological Studies: The morphological observation for synthesized SDG material is examined using different microscopy techniques shown in fig. 1. Figures 1A and 2B exhibited the SEM and FE-SEM images of SDG material revealing the crumpled sheet-like morphology having huge surface area after rapid removal of oxygen-containing

function groups followed by sulfur atom incorporation in carbon network during hydrothermal process and exfoliation process. Fig. 1C shows the HR-TEM image of synthesized SDG material exhibiting wave-like morphology which is in good agreement with formerly addressed results¹⁰.

The nature of this material might have initiated from the defective structural morphology attained throughout the S-heteroatom doping procedure³⁷. Fig. 1D showed the HR-TEM lattice fringes with an interlayer distance of 0.41 Å. These microscopy images signify that doped graphene material has defects and they may act as active sites for electrocatalysts.

Raman Spectroscopy Analysis: The finite non-destructive Raman spectroscopy technique is chiefly used to examine the structural changes for graphite and its related materials. The typical Raman spectroscopy study of synthesized graphite, graphene oxide and SDG materials is depicted in figure 2. These materials showed a prominent peak at 1366 and $1655\ cm^{-1}$ strongly equivalent to the D and G bands correspondingly^{1,31}. Moreover, the ratio of D and G bands (I_D/I_G) will provide information about the change in structural features and defects in the synthesized materials. The I_D/I_G ratio changes from each of these materials strongly indicate the proper exfoliation followed by the S atom being incorporated into the carbon network.

Fourier-Transform Infrared Spectroscopy (FT-IR) Studies: FT-IR is widely experienced technique for the determination of various functional groups. Figure 3 depicts FT-IR spectra of GO, SDG and graphite. Fig. 3 indicated that these materials demonstrated a characteristic peak about $1645\ cm^{-1}$ along with $3445\ cm^{-1}$ strongly signifying the double bond between carbon atoms (-C=C) and a hydroxyl group (-OH) respectively⁹. However, the SDG material showed a peak at $1043\ cm^{-1}$ corresponding to sulfur-bonded carbon materials, whereas this peak is not observed in other material. FT-IR result indicates that the sulfur atom is successfully incorporated into the carbon network. The possible defects after the incorporation of S-atom in SDG material play a vital role for enhancing the electrochemical activity at the interface²⁶.

X-ray Photo Electron Spectroscopy Analysis: XPS is a powerful technique to examine the elemental analysis of catalyst materials. Figure 4 shows the deconvolution S spectra of SDG material. The sulfur signal in XPS spectra is observed at binding energies of 161.4 eV and 162.6 eV depicting $2p_{3/2}$ and $2p_{1/2}$ strongly equivalent to the -C-S-C- and thiophene-S correspondingly and these outcomes are in excellent agreement by means of the previous reports^{8,23}. This XPS study indicated that the 'S' atom is efficiently doped into the carbon arrangement and this consequence is in good agreement through the Raman and IR-Spectroscopy studies. SDG was further subjected to investigate the hydrophobic or hydrophilic activity and was examined using contact angle measurements.

Fig. 5A shows the water contact angle images of SDG material and it has contact angles of 136° and 137° indicating that SDG materials have hydrophobic activity. Fig. 5B showed the emission spectra of SDG material strongly indicating that it has emission properties. A topography study of synthesis SDG catalyst was examined using AFM as depicted in fig. 5C and the corresponding height profile is described in Figure 5D. AFM study exposed that the material

is crimped morphology with a few nm height profiles and its good agreement with the FE-SEM and HR-TEM analysis.

Electrochemical Determination of Dopamine: The individual electrochemical responses of dopamine and ascorbic acid are investigated through square wave voltammetry technique using synthesized SDG and without modified GCE in 0.1 M PBS.

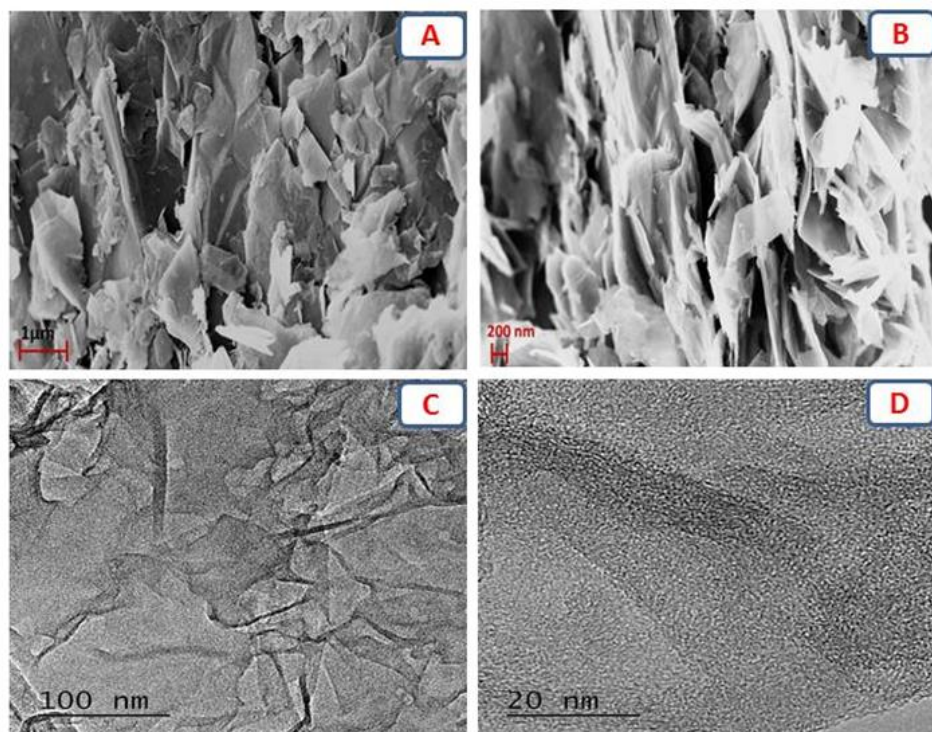


Fig. 1: (A) SEM (B) FEM-SEM images of SDG, (C) HR-TEM image of SDG (D) HR-TEM images of lattice fringes.

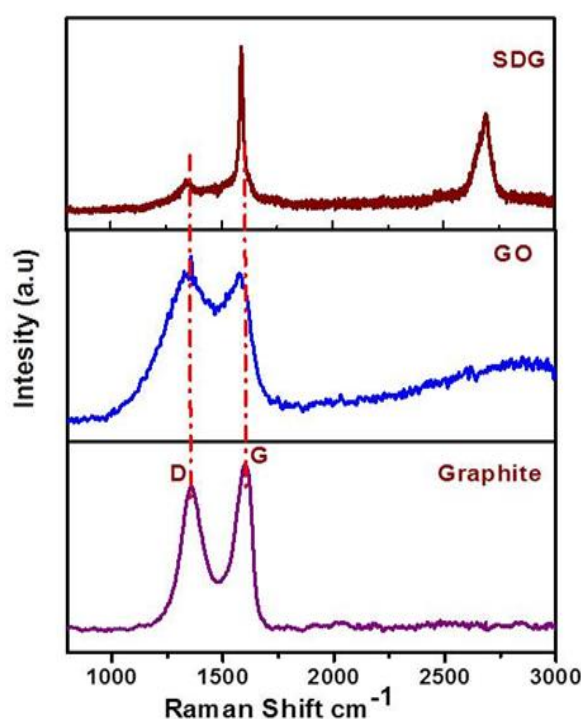


Figure 2: Raman Spectra of respective materials.

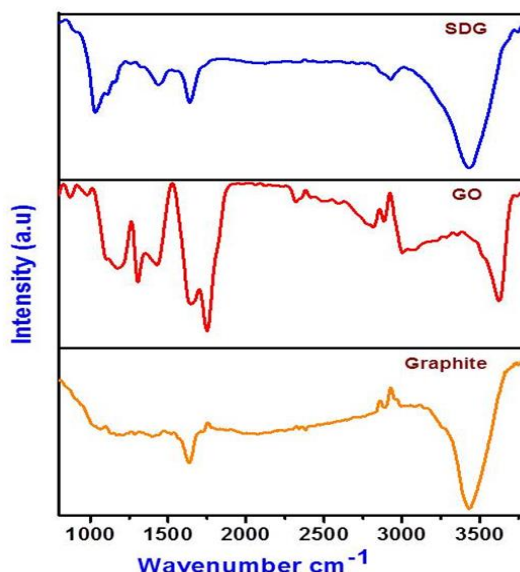


Fig. 3: FT-IR spectroscopy analysis of respective materials

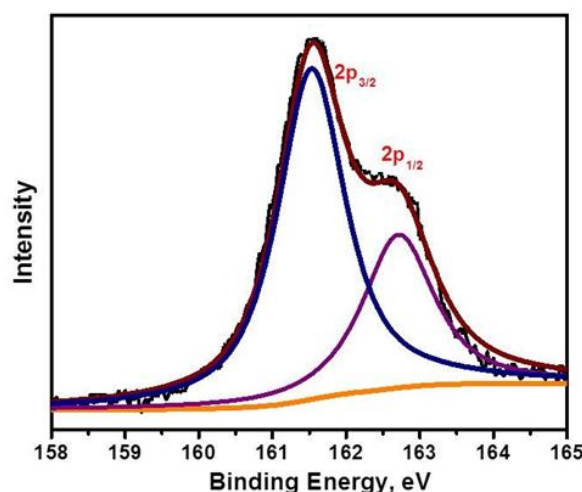
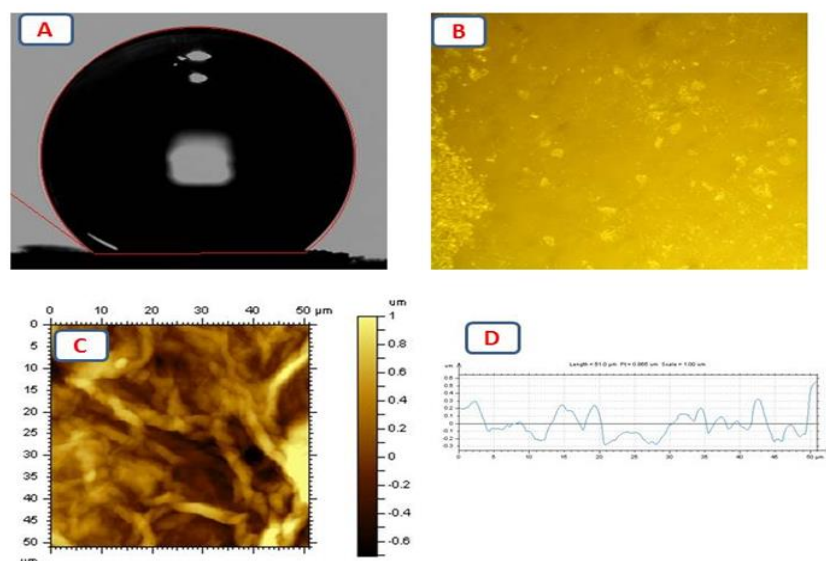
Fig. 4: High-resolution XPS spectra of S_{2p} of SGD material

Fig. 5: (A) Contact angle image, (B) Emission spectra images, (C) AFM topography and (D) Corresponding height profile of SDG material.

Voltammogram response for without modified GCE as well as modified GCE in a freshly prepared 0.1M PBS electrolyte holding 0.5 mM of DA at a scan speed of 20 mV/s is revealed in figure 6. From the figure 6, it exhibited a well-shaped square wave voltammetry for S-doped graphene-modified GCE. Compared to unmodified GCE, SDG/GCE electrode (Fig. 6a) showed higher peak current (53.2 μ A) and low overpotential (0.12V vs Ag/AgCl) than bare GCE (Fig. 6b) where having 0.13 V vs Ag/AgCl, 8.5 μ A.

The improved electrochemical activity of SDG catalyst material is attributed to the following reasons⁴²: First, high surface area, more active sites and edge planes. Secondly high conductive SDG material can improve the electron transfer properties at electrode-electrolyte interface. Finally, S-doping in the carbon network generates a more negative charge on graphene in an electrolyte solution, which increases the diffusion and adsorption of positively charged DA on the modified electrode surface.

Electrochemical Determination of Ascorbic Acid: The synthesized material is utilized for accurate identification of AA in 0.1 M PBS using SDG/GCE. The CV response for without modification of GCE and SDG/GCE of 0.5mM and

AA contains 0.1M PBS electrolyte at a scan accelerate of 20mV/s as described in figure 7. In this observation of AA, the resulted oxidation peak for AA mainly signifies the oxidation of -OH groups in -COOH groups present on furan cycliring of AA at the electrode surface. In fig. 7, SDG/GCE (Fig.7b) is having high oxidation peak current with a value of 9 μ A and a low over potential 1.69 V vs Ag/AgCl compared to bare GCE (Fig. 7a)^{19,22}.

The enhanced electrochemical response for SDG materials is owing to the development of hydrogen bonds among the ascorbate and graphene material in SDG catalyst and high surface area, more active sites and edge planes. So, S-doping in graphene can enhance the charge transfer properties at the electrode-electrolyte interface and drastically minimizes the over potential of AA oxidation as well.

In addition to this, we carried out the cause of pH using 0.1M PBS on the electrochemical activity of DA and AA recorded in a series of pH solutions using SDG/GCE as shown in fig. 8. The results are indicated by the oxidation of peak current of DA (Fig. 8A) as well as AA (Fig. 8B), enhanced by increasing the pH value from of pH 4 to pH 7 followed by decrease from pH 7 to pH 9.

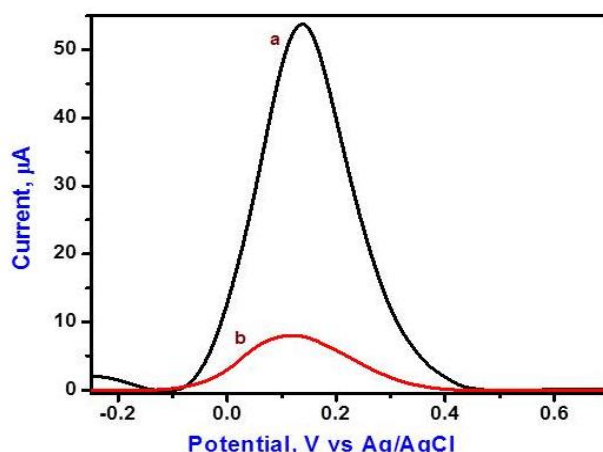


Fig. 6: (a) square wave voltammetry response of the Bare GCE (b) SDG/GCE in 0.1M PBS holding 0.5 mM of DA at a scan speed of 20 mV/s.

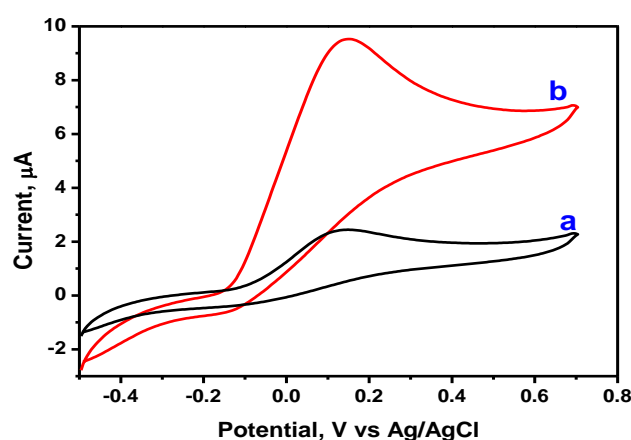


Fig. 7: Cyclic voltammogram response of 0.3mM AA in 0.1M PBS at SDG/GCE and without modification of GCE at a scan accelerate of 50 mV/s

The oxidation peak current reached a maximum at a pH value of 7. In addition to this, this pH is a physically suitable value and it can also be used for real-time applications.

Therefore, based on these observations, 0.1M PBS supporting electrolyte is used at pH 7 for all the electrochemical experiments. Further chronoamperometry

(CA) experiments were carried out to accurate determination of DA in 0.1M PBS electrolyte. The CA response of the SDG/GCE to DA was investigated by successive addition of DA to continuous stirring of PBS electrolyte under optimized conditions (pH 7.0 and applied potential 0.16V vs Ag/AgCl).

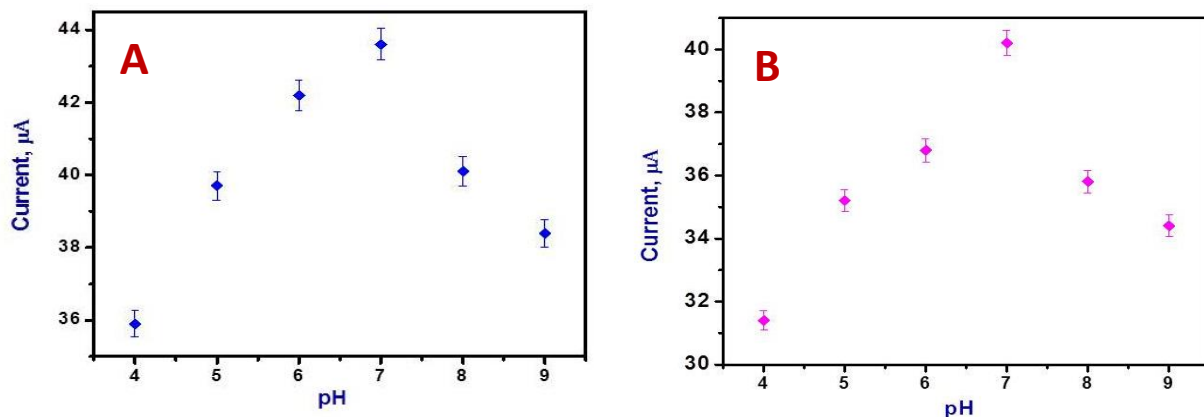


Fig. 8: Result of pH on the peak current of SDG/GCE for (A) DA and (B) AA in 0.5 mM containing 0.1M PBS electrolyte

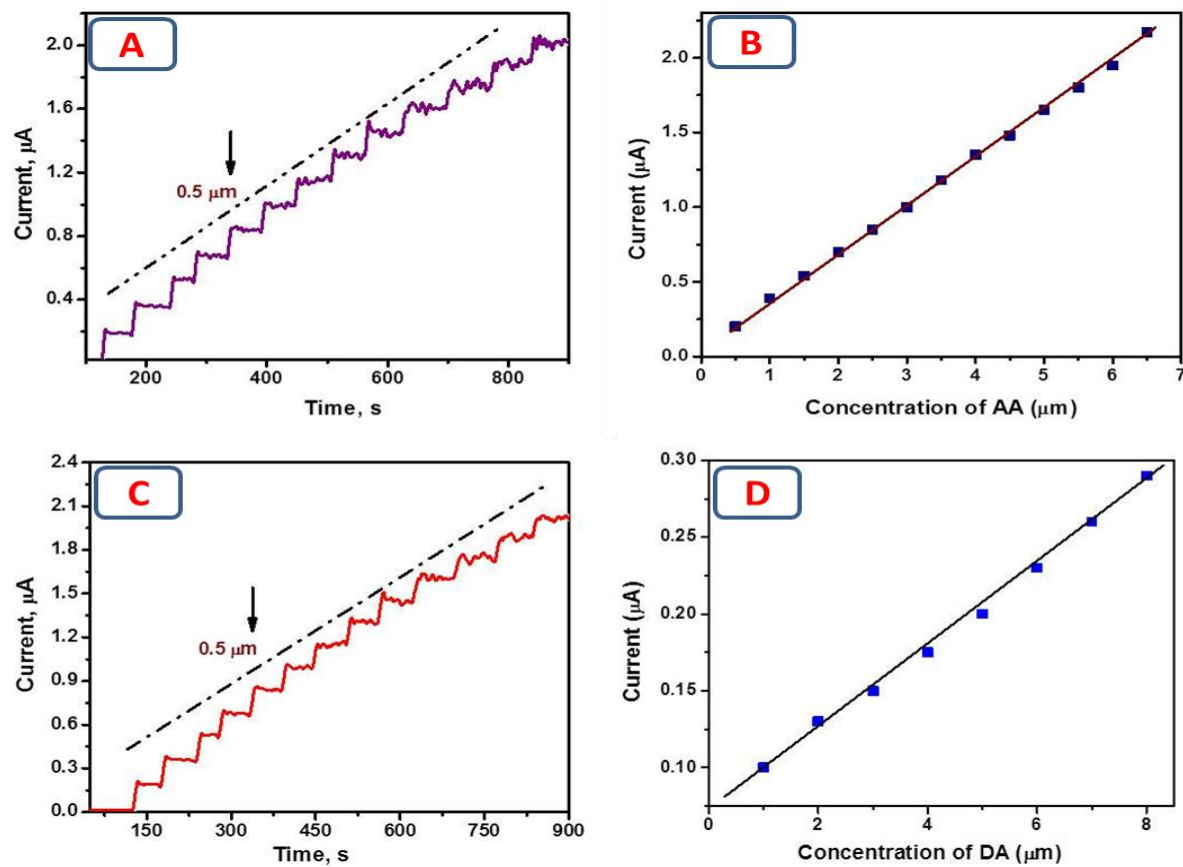


Fig. 9: (A) The current time observation of SDG/GCE under continuous stirring condition for the consecutive addition of $0.5\mu\text{M}$ DA to the 0.1M PBS electrolyte at applied potentials of 0.16V. (B) Showing the respective calibration plot of A. (C) The current time observation of SDG/GCE under continuous stirring conditions for the consecutive addition of $0.5\mu\text{M}$ AA to the 0.1M PBS electrolyte at applied potentials of 1.69 V (D) Illustrating the respective calibration plot of A.

Fig. 9A showed the current-time response for successive addition of $0.5\mu\text{m}$ from standard stock solution after certain intervals. It is shown that after each addition of DA, the current is drastically improved and the maximum reached its steady state response less than 3s. Fig. 9B is the plot for catalytic response changing linearly with the DA concentration of 0.5 - $6.5\mu\text{m}$ by means of a linear correlation coefficient (R^2)-0.99. Then the sensitivity of SDG/GCE is $0.33\mu\text{A}/\mu\text{m}$ and the limit of detection is $0.36\mu\text{m}$. Further, CA analysis is carried out by successive addition of AA using SDG/GCE. Fig. 9C illustrated the classic CA reaction of SDG/GCE to the consecutive addition of $0.5\mu\text{m}$ of AA into the stirring 0.1M PBS with constant time intervals.

After each injection of AA, the oxidation peaks current sharply increased followed by its maximum steady-state current response within 3s, this strongly signifies that rapid adsorption and activation of AA on SDG/GCE surface and fast charge transfer properties by the electrode-electrolyte interface. The corresponding calibration plot shown in fig. 9D exhibited a finite relationship of current *vs* the AA concentration in the range of 0.5 to $6.5\mu\text{m}$ with a correlation coefficient value (R^2) of 0.99 (S/N-3) resulting from the calibration curve and the calculated sensitivity of $0.22\mu\text{A}/\mu\text{m}$ with a limit of detection $0.30\mu\text{m}$. From this

analysis, it was clearly shown the SDG/GCE exhibited finite AA finding performance with a low limit of detection, sensitivity, as well as moderate linear range.

The simultaneous identification of DA and AA in the mixture is examined by employing the CV procedure utilizing the proposed 0.1M PBS containing SDG/GCE. In the experimentation performed, concentration of the AA compound is close two-fold higher than DA and these results are shown in Fig. 10. Fig. 10a showed that the electrochemical response of bare GCE does not show the instantaneous simultaneous estimation of AA and DA, however after modification with SDG material (Fig. 10b), it showed two oxidation peaks for AA and DA respectively by means of a peak to peak to the difference of 0.26 V *vs* Ag/AgCl . The electrocatalytic property of developed SDG/GCE is arising due to high surface area and active sites.

Stability test: Further, the extended stability of the proposed SDG/GCE sensor was examined for the long time period of 12-day as illustrated in figure 11. The results described that the oxidation peak current response is stable more than 95% even after two weeks, suggesting that the developed sensor is also useful for real-time applications.

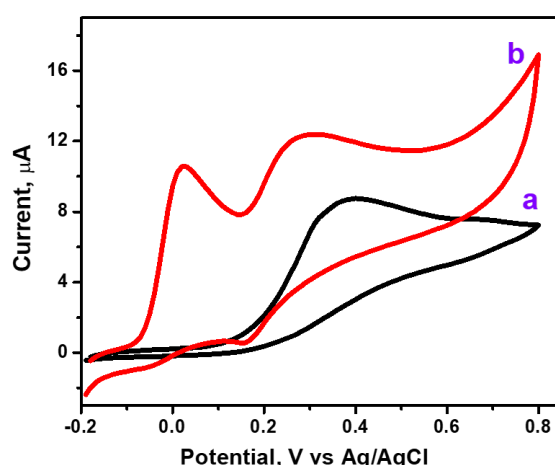


Fig. 10: CV of a mixture of 1mM of DA and 0.3 mM of AA containing 0.1M PBS using SDG/GCE at a scan rate of 50mV/s.

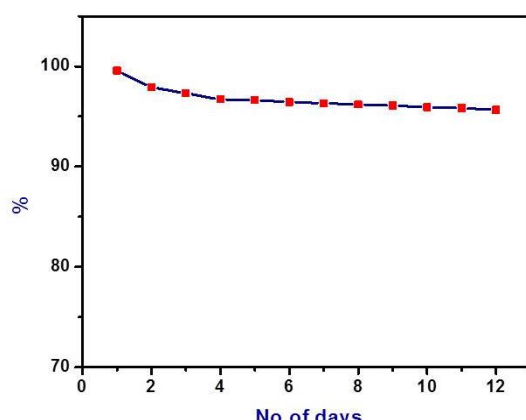


Fig. 11: Stability test of SDG/GCE

Conclusion

A novel electrochemical sensor platform was developed using S-doped graphene-supported GCE for the accurate estimation of DA and AA, along through their simultaneous determination using various electroanalytical techniques at room temperature. The results demonstrated significant improvements in charge transfer properties at the electrode-electrolyte interface. The proposed SDG/GCE sensor exhibited finite selectivity, superior sensitivity, a moderate bound of detection and long-standing stability. This innovative nanomaterial-based sensor shows a promising sensor platform for the advancement of electrochemical (bio) sensors.

Acknowledgement

The authors are grateful to the management of Nanosol Energy Pvt. Ltd., Hyderabad, India, for their constant support and encouragement.

References

1. Ahmed M.S., Han H.S. and Jeon S., One-step chemical reduction of graphene oxide with oligothiophene for improved electrocatalytic oxygen reduction reactions, *Carbon*, **61**, 164-172 (2013)
2. Arrigoni O. and De Tullio M.C., Ascorbic acid: Much more than just an antioxidant, *Biochimica et Biophysica Acta (BBA)-General Subjects*, **1569**(1-3), 1-9 (2002)
3. Ates M., Castillo J., Sezai Sarac A. and Schuhmann W., Carbon fiber microelectrodes electrocoated with polycarbazole and poly (carbazole-co-p-tolylsulfonyl pyrrole) films for the detection of dopamine in the presence of ascorbic acid, *Microchimica Acta*, **160**, 247-251 (2008)
4. Chen J., Zhang J., Lin X., Wan H. and Zhang S., Electrocatalytic Oxidation and Determination of Dopamine in the Presence of Ascorbic Acid and Uric Acid at a Poly (4-(2-Pyridylazo)-Resorcinol) Modified Glassy Carbon Electrode, *Electroanalysis: An International Journal Devoted to Fundamental and Practical Aspects of Electroanalysis*, **19**(5), 612-615 (2007)
5. Cline K.K., Baxter L., Lockwood D., Saylor R. and Stalzer A., Nonaqueous synthesis and reduction of diazonium ions (without isolation) to modify glassy carbon electrodes using mild electrografting conditions, *Journal of Electroanalytical Chemistry*, **633**(2), 283-290 (2009)
6. Darabi R. et al, Simultaneous determination of ascorbic acid, dopamine and uric acid with a highly selective and sensitive reduced graphene oxide/polypyrrole-platinum nanocomposite modified electrochemical sensor, *Electrochimica Acta*, **457**, 142402 (2023)
7. Deng C., Chen J., Wang M., Xiao C., Nie Z. and Yao S., A novel and simple strategy for selective and sensitive determination of dopamine based on the boron-doped carbon nanotubes modified electrode, *Biosensors and Bioelectronics*, **24**(7), 2091-2094 (2009)
8. Díaz J., Paolicelli G., Ferrer S. and Comin F., Separation of the sp₃ and sp₂ components in the C1s photoemission spectra of amorphous carbon films, *Phys. Rev. B*, **54**, 8064 (1996)
9. Ferrari A.C., Meyer J.C., Scardaci V., Casiraghi C., Lazzeri M., Mauri F., Piscanec S., Jiang D., Novoselov K.S., Roth S. and Geim A.K., Raman Spectrum of Graphene and Graphene Layers, *Phys. Rev. Lett.*, **97**, 187401 (2006)
10. Gao W., Alemany L.B., Ci L.J. and Ajayan P.M., New insights into the structure and reduction of graphite oxide, *Nat. Chem.*, **1**, 403-408 (2009)
11. Giddaerappa K., Naseem K., Shivalingayya G. and Lokesh K.S., Macromolecule–Nanoparticle-Based Hybrid Materials for Biosensor Applications, *Biosensors*, **14**(6), 277 (2024)
12. Girma Salale G., Recent advances in electrochemical sensors based on molecularly imprinted polymers and nanomaterials for detection of ascorbic acid, dopamine and uric acid, *Sens. Bio-Sens. Res.*, **43**, 100610 (2024)
13. Heien M.L., Khan A.S., Ariansen J.L., Cheer J.F., Phillips P.E., Wassum K.M. and Wightman R.M., Real-time measurement of dopamine fluctuations after cocaine in the brain of behaving rats, *Proceedings of the National Academy of Sciences*, **102**(29), 10023-10028 (2005)
14. Hou S., Kasner M.L., Su S., Patel K. and Cuellar R., Graphene and Its Derivatives-Based Biosensing System, *J Phys Chem C*, **114**(35), 14915-21 (2010)
15. Huang J., Liu Y., Hou H. and You T., Simultaneous electrochemical determination of dopamine, uric acid and ascorbic acid using palladium nanoparticle-loaded carbon nanofibers modified electrode, *Biosensors and Bioelectronics*, **24**(4), 632-637 (2008)
16. Jia N., Wang Z., Yang G., Shen H. and Zhu L., Electrochemical properties of ordered mesoporous carbon and its electroanalytical application for selective determination of dopamine, *Electrochemistry Communications*, **9**(2), 233-238 (2007)
17. Li D., Müller M.B., Gilje S., Kaner R.B. and Wallace C.G., Processable aqueous dispersions of graphene nanosheets, *Nat. Nanotechnol.*, **3**, 101 (2008)
18. Liu J., Tang J. and Gooding J.J., Strategies for chemical modification of graphene and applications of chemically modified graphene, *J Mater Chem*, **22**(25), 12435-52 (2012)
19. Liu Q., Zhu X., Huo Z., He X., Liang Y. and Xu M., Electrochemical detection of dopamine in the presence of ascorbic acid using PVP/graphene modified electrodes, *Talanta*, **97**, 557-562 (2012)
20. Liu Y., Dong X. and Chen P., Biological and chemical sensors based on graphene materials, *Chem Soc Rev*, **41**(6), 2283-307 (2012)
21. Liu Y. et al, Simultaneous determination of dopamine, ascorbic acid and uric acid with an electrospun carbon nanofibers modified electrode, *Electrochemistry Communications*, **10**(10), 1431-1434 (2008)
22. Min K. and Yoo Y.J., Amperometric detection of dopamine based on tyrosinase-SWNTs-Ppy composite electrode, *Talanta*, **80**, 1007-1011 (2009)

23. Mohammad A., Khan M.E. and Cho M.H., Sulfur-doped-graphitic-carbon nitride (Sg-C₃N₄) for low-cost electrochemical sensing of hydrazine, *Journal of Alloys and Compounds*, **816**, 152522 (2020)

24. Musa Farkad Hawas, Hussen Noor Mohammed, Hasan Anmar Nazar and Salih Thaer Abdulqader, Bacterial plasmid: A study of its role in resistance to some antibiotics and natural substances, *Res. J. Biotech.*, **19(11)**, 35-41 (2024)

25. Nagles E., Riesco F. and Roldan-Tello L., Electrochemical Determination of Dopamine with a Carbon Paste–Lanthanum (III) Oxide Micro-Composite Electrode: Effect of Cetyl Trimethyl Ammonium Bromide Surfactant Selectivity, *Sensors*, **24(16)**, 5420 (2024)

26. Poh H.L., Simek P., Sofer Z.K. and Pumera M., Sulfur-doped graphene via thermal exfoliation of graphite oxide in H₂S, SO₂, or CS₂ gas, *ACS Nano*, **7(6)**, 5262–72 (2013)

27. Prasad K.S., Muthuraman G. and Zen J.M., The role of oxygen functionalities and edge plane sites on screen-printed carbon electrodes for the simultaneous determination of dopamine, uric acid and ascorbic acid, *Electrochemistry Communications*, **10(4)**, 559-563 (2008)

28. Shervedani R.K., Bagherzadeh M. and Mozaffari S.A., Determination of dopamine in the presence of high concentrations of ascorbic acid by using gold cysteamine self-assembled monolayers as a nanosensor, *Sensors and Actuators B: Chemical*, **115(2)**, 614-621 (2006)

29. Thiagarajan S. and Chen S.M., Preparation and characterization of PtAu hybrid film modified electrodes and their use in simultaneous determination of dopamine, ascorbic acid and uric acid, *Talanta*, **74(2)**, 212-222 (2007)

30. Wang Q., Wen X. and Kong J., Recent progress on uric acid detection: a review, *Critical Reviews in Analytical Chemistry*, **50(4)**, 359-375 (2020)

31. Wang S., Zhang L., Xia Z., Roy A., Chang D.W. and Baek J.B., BCN graphene as efficient metal-free electrocatalyst for the oxygen reduction reaction, *Angew Chem Int Ed*, **51(17)**, 4209–12 (2012)

32. Wightman R.M., May L.J. and Michael A.C., Detection of dopamine dynamics in the brain, *Analytical Chemistry*, **60(13)**, 769A-793A (1988)

33. Xu T.Q., Zhang Q.L., Zheng J.N., Lv Z.Y., Wei J., Wang A.J. and Feng J.J., Simultaneous determination of dopamine and uric acid in the presence of ascorbic acid using Pt nanoparticles supported on reduced graphene oxide, *Electrochimica Acta*, **115**, 109-115 (2014)

34. Yang H., Zhao J., Qiu M., Sun P., Han D., Niu L. and Cui G., Hierarchical bi-continuous Pt decorated nanoporous Au-Sn alloy on carbon fiber paper for ascorbic acid, dopamine and uric acid simultaneous sensing, *Biosensors and Bioelectronics*, **124**, 191-198 (2019)

35. Yang L., Liu D., Huang J. and You T., Simultaneous determination of dopamine, ascorbic acid and uric acid at an electrochemically reduced graphene oxide modified electrode, *Sensors and Actuators B: Chemical*, **193**, 166-172 (2014)

36. Yang S., Liu X., Zeng X., Xia B., Gu J., Luo S., Mai N. and Wei W., Fabrication of nano-copper/carbon nanotubes/chitosan film by one-step electrodeposition and its sensitive determination of nitrite, *Sensors and Actuators B: Chemical*, **145(2)**, 762-768 (2010)

37. Yang S.B., Zhi L.J., Tang K., Feng X.L., Maier J. and Mullen K., Efficient Synthesis of Heteroatom (N or S)-Doped Graphene Based on Ultrathin Graphene Oxide-Porous Silica Sheets for Oxygen Reduction Reactions, *Adv. Funct. Mater.*, **22**, 3634-3640 (2012)

38. Yao H., Sun Y., Lin X., Tang Y. and Huang L., Electrochemical characterization of poly (eriochrome black T) modified glassy carbon electrode and its application to simultaneous determination of dopamine, ascorbic acid and uric acid, *Electrochimica Acta*, **52(20)**, 6165-6171 (2007)

39. Yasmin S., Ahmed M.S. and Jeon S., Determination of dopamine by dual-doped graphene-Fe₂O₃ in the presence of ascorbic acid, *Journal of The Electrochemical Society*, **162(14)**, B363 (2015)

40. Yen G.C., Duh P.D. and Tsai H.L., Antioxidant and pro-oxidant properties of ascorbic acid and gallic acid, *Food Chemistry*, **79(3)**, 307-313 (2002)

41. Zare H.R., Nasirizadeh N. and Ardakani M.M., Electrochemical properties of a tetrabromo-p-benzoquinone modified carbon paste electrode. Application to the simultaneous determination of ascorbic acid, dopamine and uric acid, *Journal of Electroanalytical Chemistry*, **577(1)**, 25-33 (2005)

42. Zhang L., Niu J., Li M. and Xia J.Z., Catalytic Mechanisms of Sulfur-Doped Graphene as Efficient Oxygen Reduction Reaction Catalysts for Fuel Cells, *J. Phys. Chem. C*, **118**, 3545–3553 (2014)

43. Zhang Y., Pan Y., Su S., Zhang L., Li S. and Shao M., A novel functionalized single-wall carbon nanotube modified electrode and its application in the determination of dopamine and uric acid in the presence of high concentrations of ascorbic acid, *Electroanalysis: An International Journal Devoted to Fundamental and Practical Aspects of Electroanalysis*, **19(16)**, 1695-1701 (2007)

44. Zhao Y., Gao Y., Zhan D., Liu H., Zhao Q., Kou Y., Shao Y., Li M., Zhuang Q. and Zhu Z., Selective detection of dopamine in the presence of ascorbic acid and uric acid by a carbon nanotubes-ionic liquid gel modified electrode, *Talanta*, **66(1)**, 51-57 (2005).

(Received 09th April 2025, accepted 13th May 2025)